The thalamus is a gateway for stimulus-evoked activity in the habenula

◆Ruey-Kuang Cheng[1], ◆Seetha Krishnan[2], Qian Lin[2], David G. C. Hildebrand[3, 4], Isaac H. Bianco[4], Caroline Kibat[1] and *Suresh Jesuthasan[1,5, 6, 7]

[1]Neural Circuitry and Behavior Laboratory, Institute of Molecular and Cell Biology, Singapore 138673.

[2]NUS Graduate School for Integrative Sciences and Engineering, 28 Medical Drive, National University of Singapore, Singapore 117456.

[3]Graduate Program in Neuroscience, Division of Medical Sciences, Graduate School of Arts and Sciences, Harvard University, Cambridge, Massachusetts 02138 United States of America.

[4]Department of Molecular and Cell Biology, Harvard University, Cambridge, Massachusetts 02138, United States of America.

[5]Lee Kong Chian School of Medicine, Nanyang Technological University, Singapore

[6]Neuroscience and Behavioral Disorders Program, Duke-NUS Graduate Medical School, 8 College Road, Singapore 169857.

[7]Department of Physiology, National University of Singapore, Singapore 117597.

*Corresponding author: sureshjj@imcb.a-star.edu.sg; +65 65869545

◆equal contribution

Abstract

The thalamus receives input from multiple brain systems and has an essential role in controlling brain state. This is thought to occur primarily because of its connectivity with the forebrain. Here, we provide evidence for an additional mechanism. By calcium imaging of larval zebrafish, we show that two stimuli – light and darkness - trigger distinct activity patterns in the habenula. Responses appear first in a neuropil that is innervated by retino-recipient thalamic nuclei. Thalamic responses to light and darkness resemble habenula responses, and the thalamus appears to be the only source of GABAergic afferents that would underlie the inhibitory component of light-evoked activity. These data establish that the thalamus directly controls the habenula, a regulator of many broadly acting neuromodulators. We thus propose that the thalamus influences brain state via a pathway to the habenula, which can act in parallel with projections to the forebrain.

Introduction

Sensory stimuli affect animal behavior by enabling perception and also by changing brain state. Light, for example, allows objects to be seen, but can also affect mood (Vandewalle et al. 2010), alertness (Badia et al. 1991), cognitive ability (LeGates et al. 2012) and movement (Aschoff 1960; Burgess & Granato 2007), with different wavelengths having different effects (Vandewalle et al. 2010). Light processing usually begins in the eyes, which contains rods and cones and project to centers in the brain via diverse retinal ganglion cells (RGCs) (Baden et al. 2016). In addition, light is detected by melanopsin-expressing RGCs that are maximally sensitive to blue light, and these have a role in behavior that is independent of image formation (Hattar et al. 2003; Provencio et al. 2002). How signals from light sensors influence a range of brain functions remains

unclear (Chellappa et al. 2011). One route could be via the release of neuromodulators, which have an essential role in selecting the functional connectivity in neural circuits, and thereby altering brain state (Marder 2012; Bargmann & Marder 2013; Getting 1989). Indeed, the ability of light to affect normal movement patterns (Burgess et al. 2010) or to disrupt mood and cognition (LeGates et al. 2012) involves serotonin. An intriguing question thus is how neuromodulator release is tailored to lighting conditions.

The habenula is an evolutionarily conserved structure in the epithalamus (Stephenson-Jones et al. 2012), which controls the release of neuromodulators that have broad effects on the brain, such as serotonin, dopamine, epinephrine and histamine (Jhou et al. 2009; Quina et al. 2014; Morley et al. 1985; Wang & Aghajanian 1977). Light-evoked activity has been detected in the habenula of several different species, including the rat (Zhao & Rusak 2005), pigeon (Semm & Demaine 1984) and zebrafish (Dreosti et al. 2014). The habenula is divided into two subdomains, termed dorsal and ventral in fish, or medial and lateral in mammals. These are defined on the basis of their afferent neurons and projection targets (Okamoto et al. 2012). In the rat and pigeon, electrophysiological recording was used to demonstrate that light triggers both excitation and inhibition in the habenula. Evoked activity, either phasic or sustained, was detected in both medial and lateral subdomains. The pathways mediating this activity are unknown. In zebrafish, flashes of red light excite the dorsal left habenula, with additional activity apparent bilaterally in the ventral habenula (Dreosti et al. 2014). This activity is dependent on the eyes, but how the light detection by the eyes influences habenula activity is again unknown.

Zebrafish can detect light, but are also sensitive to the loss of light. Sudden darkness triggers a startle response (Easter & Nicola 1996), while gradual reductions in light cause turning (Burgess & Granato 2007) and dark regions of a tank are usually

avoided by larval zebrafish in a serotonin-dependent manner (Cheng et al. 2016; Steenbergen et al. 2011). Reduction in luminance has also been shown to affect the habenula (Bianco & Engert 2015; Portugues et al. 2014). We show that the thalamus may control both light- and dark-evoked responses. This paper therefore establishes how illumination conditions affect the habenula, and in doing so, demonstrates a new functional connection of the thalamus, a structure that is better characterized for its functions in cognition and brain state control via projections to telencephalic structures (Sherman & Guillery 2002; Mitchell et al. 2014; S.-H. Lee & Dan 2012).

Results

Light and darkness trigger activity in the habenula

The zebrafish habenula consists of neurons surrounding neuropils that are innervated by afferent neurons (Hendricks & Jesuthasan 2007; Miyasaka et al. 2009; Amo et al. 2014). To identify the pathways by which light influences the habenula, we first characterized habenula activity evoked by illumination changes. Two-photon imaging was performed on a transgenic zebrafish line expressing the calcium indicator GCaMP3 in the habenula (Krishnan et al. 2014) (Figure 1A). Resonant-scanning, combined with piezo-driven focusing, was used to record the activity of cells at multiple focal planes throughout the habenula (Figure 1B, C). With a step size of 10 μm, so that each cell would be sampled only once, most of the habenula could be covered with 5 planes at a rate of 1 Hz. Habenula activity was monitored as the larva was exposed to discrete pulses of blue light. Evoked activity – both transient and sustained - was detected throughout the habenula (Figure 1D, E). This activity was reproducible, as shown by the trajectory of the system through state space (Figure 1F). Similar responses were seen an analysis of 6 fish. A minority of cells displayed a sustained decrease in

fluorescence during light ON, suggesting inhibition by light (Figure 1G). These observations confirm that the activity of zebrafish habenula neurons is affected by light, and that in addition to excitation there is inhibition by light and excitation during darkness.

Light-evoked activity occurs first in the dorsal left neuropil

To obtain a finer time-course of light evoked activity, we used higher speed (13 - 100 Hz) microscopy of fish expressing GCaMP3 (Figure 2A-F) in the habenula. With widefield imaging, the excitation light triggered a response first in the dorsal left neuropil and then in cells throughout the habenula, including lateral regions that correspond to the ventral habenula. To examine the response to light offset, two-photon imaging was used. Onset and offset of light evoked a response in different regions of the dorsal left neuropil (Fig. 2G, H). Increasing the intensity of illumination led to a stronger response in the neuropil and excitation in more cells (Figure 2I, J). These observations are consistent with the existence of non-overlapping sources of input neurons to the dorsal left neuropil for light and darkness.

The parapineal is not required for blue light responses in the dorsal left neuropil

The dorsal left neuropil is directly innervated by the parapineal (Fig. 3A), a light-sensitive structure. Although the opsins present in the zebrafish parapineal have not been described, parapinopsin has been found in the catfish parapineal (Blackshaw & Snyder 1997) and zebrafish parapinopsin PP2 is maximally sensitive to blue light (Koyanagi et al. 2015). The parapineal is not required for detection of flashes of red light in zebrafish (Dreosti et al. 2014). It could, however, mediate the blue light response. To test this, the parapineal was laser ablated in the *Et(SqKR4)* line (Fig. 3B, C). Blue light-evoked activity in the habenula was not eliminated following parapineal lesion (Fig. 3D-F), however, suggesting that other inputs could exist.

The thalamus provides a source of input to the dorsal left neuropil

The entopeduncular nucleus (EN) is the major source of habenula afferents in teleosts (Yañez & Anadon 1994), including zebrafish (Amo et al. 2014). This nucleus is labeled in the *Et(sqKR11*) line (A. Lee et al. 2010), providing a simple way of visualizing afferents to the habenula. The intensity of fluorescent label in the dorsal left neuropil is relatively low in comparison to other neuropils (Figure 4A), suggesting that there may be fewer EN neurons that terminate in this neuropil. It is possible that there is innervation by an EN subpopulation is largely unlabeled in the *Et(sqKR11)* line. An alternative possibility is that there is another source of afferents to this neuropil. To test this, the lipophilic tracer DiD was injected into the dorsal left neuropil (n = 6 fish). In all cases, neurons in the dorsal left habenula (which extend dendrites into the neuropil), the parapineal, and a thalamic nucleus located ventrally to both habenula (Figure 4B-E) were labelled. DiD label was not detected in any other regions of the brain, and only rarely in the entopeduncular nucleus (Figure 4C), suggesting that the thalamus is the major source of input to the dorsal left neuropil. The label in the thalamus cannot represent anterograde label from the habenula, as tracing of projections from the habenula by expressing fluorescent proteins specifically in the habenula does not result in a projection to the dorsal thalamus (Movie S1). Moreover, the labeling of cell bodies (Figure 4D) indicates that this is likely to be a retrograde label. The neuropil of this thalamic nucleus contains terminals of retinal ganglion cells, as shown by DiI injection into the retina (Fig. 4F). Based on the location of these terminals relative to the optic tract, these terminals make up AF2 and AF4 (Easter & Nicola 1996; Robles et al. 2014). Thus, the habenula neuropil with the initial response to light is innervated by thalamic nuclei that receive retinal input.

The habenula receives glutamatergic and GABAergic input from the thalamus

Light caused both excitation and inhibition in zebrafish habenula neurons, implying that there should be excitatory and inhibitory afferents. Using an antibody to vGlut1/2, glutamatergic pre-synapses were detected the dorsal left neuropil (Figure 4G), indicating the existence of excitatory afferents. GAD65/67 labeled puncta could also be detected in the dorsal left neuropil (Figure 4H). Dimmer label was seen in other neuropils, while in the lateral regions, corresponding to the ventral habenula, streaks were detected adjacent to cell bodies. We could not find any GABAergic cell bodies in the habenula, implying that these puncta and streaks must reside in habenula afferents (i.e. axon terminals). Consistent with this, inhibitory neurons could be detected in the dorsal thalamus, using a transgenic line, *Tg(gad1b:RFP, vGlut2a:GAL4, UAS:eGFP)* (Satou et al. 2013) (Figure 4I). No label was seen in the entopeduncular nucleus, which has previously been shown to be glutamatergic (Amo et al. 2014). These observations confirm that the thalamus contains both GABAergic and glutamatergic neurons, as described previously (Mueller 2012), which may mediate light-evoked excitation and inhibition of habenula neurons.

Activity in the thalamus resembles habenula response

If the thalamus provides afferents mediating illumination-dependent information to the habenula, there should be non-overlapping responses to light and darkness, and intensity-dependent activity here. To test this, calcium imaging was carried out using a line with broad expression of the calcium indicator GCaMP6f. A response to light was detected in the neuropil of the thalamus and in scattered cells (Figure 5A-I). Darkness triggered an increase in fluorescence in the anterior domain of the neuropil and in a different subset of thalamic neurons. Phasic and sustained responses were detected, as

found in the habenula (Figure 5G and Figure 1). Increasing the intensity of light led to an increase in the thalamic response (Figure 5J-M). The thalamus thus has different neurons responding to light ON and OFF, and an intensity-dependent response to blue light. This is consistent with the hypothesis that the thalamus mediates light-evoked activity in the habenula.

Discussion

This paper identifies a pathway by which the habenula can be controlled by light and darkness. Responses to these stimuli occur throughout the habenula, but appear initially in the dorsal left neuropil. It is unclear at present how activity spreads within the habenula – gap junctions have been reported (Jabeen & Thirumalai 2013), and there may also be local networks (Kim & Chang 2005). Since light-evoked activity begins in a neuropil, rather than a habenula neuron, it is unlikely that the responses are caused by photosensitive cells within the habenula, even though the opsin *valopb* has been detected here (Kojima et al. 2008). The parapineal also does not appear to be an essential source of blue light-evoked activity, as previously shown for red light. Rather, activity seems to be caused by bilateral input from the thalamus. Neural tracing indicates that the thalamus directly innervates the habenula, while calcium imaging shows that stimulus evoked-activity in the thalamus has features that match with stimulus evoked-activity in the habenula. Thus, by anatomical tracing and calcium imaging, our data establish a functional link from the thalamus to the habenula in zebrafish.

The region of the thalamus mediating activity in the habenula can be functionally separated into two domains, based on the response to light – excitation to light OFF in the anterior and excitation to light ON more posteriorly. The neuropil of the thalamus contains two previously defined targets of retinal ganglion cells - AF2 and AF4 (Burrill &

Easter 1994), and would thus correspond to first-order nuclei. AF4 is innervated predominantly by M3 and M4 retinal ganglion cells (Robles et al. 2014), which extend their dendritic tree into the proximal layer of the inner plexiform layer and are considered ON neurons. AF2 is innervated by B1 retinal ganglion cells that have dendrites in the distal layer (Robles et al. 2014), and these may account for the OFF responses in the thalamus and habenula. The nucleus containing AF4 may correspond to the anterior thalamus, while AF2 may correspond to a ventral nucleus (Mueller 2012; Northcutt & Wullimann 1988), implying that the habenula is innervated by more than one thalamic nucleus.

The vertebrate thalamus receives information from virtually all regions of the brain including sensory systems, motor systems, basal ganglia and cerebellum (Ward 2013). It is considered a gateway to consciousness due to its output to the cortex (Newman 1995; Crick & Koch 2003). A role in emotion has also been suggested, because of connectivity with the amygdala and hippocampus. The data here demonstrate the existence of functional connectivity between the thalamus and the habenula in zebrafish. Anatomical connectivity from the thalamus to the habenula has been reported in other vertebrates, such as amphibians (Díaz & Puelles 1992) and mammals including rabbits (Cragg 1961) and humans (Marburg 1944). Hence, this pathway is conserved in vertebrate evolution, although its functional significance has not been explored previously.

We suggest that one function of the thalamus, in addition to the well-established roles in cognition and arousal, is regulation of neuromodulator release via its projection to the habenula. Given the ability of habenula-regulated neuromodulators such as serotonin and dopamine to broadly affect neural circuits, this pathway provides a route for the control of functional connectivity by neural systems that innervate the appropriate nuclei of the thalamus, which in the case of humans includes the anterior thalamus

(Marburg 1944). We also propose that this pathway provides a potential mechanism for co-morbidity in conditions such as epilepsy and schizophrenia. Both are linked to the thalamus (Fisher & Velasco 2014; Young et al. 2000), and their major symptoms such as loss of motor control, absence seizures or hallucinations are likely due to connectivity with the forebrain. However, there are substantial cases of co-morbidity with anxiety, depression and substance abuse (Buckley et al. 2009; Muller et al. 2004; Kanner 2003; Kanner 2011). Given the involvement of the habenula in these latter disorders (Hikosaka 2010; Proulx et al. 2014; A. Lee et al. 2010; Agetsuma et al. 2010), co-morbidity may be caused by defects that involve the parallel connection with the habenula. We thus suggest that the functional connectivity identified in this paper is relevant to understanding how brain state is altered under normal conditions and also in mental illness.

Materials and Methods

Fish lines

Experiments were approved by the Institutional Animal Care and Use Committee of the Biological Resource Centre at Biopolis, Singapore. Zebrafish (*Danio rerio*) lines used for this study were: *Tg(UAS:GCaMP6s)sq202*, SqKR11Et, SqKR4Et, *s1011tEt*, Tg(UAS:GCaMP3)sq200, *Tg(elavl3:GCaMP6f)a12200* and AB wildtype.

Tg(elavl3:GCaMP6f)a12200 was generated by PCR amplification of the GCaMP6f open reading frame (Addgene plasmid 40755 (Chen et al. 2013)) with forward primer ataACTAGTgccaccATGGGTTCTCATCATCAT and reverse ataCCGCGGcTCACTTCGCTGTCATCATTTGTAC (restriction site and coding sequences in upper case, respectively). This fragment was cloned into a plasmid with Tol2 arms flanking an upstream attR1-R2 cassette and the insertion site using restriction

enzymes SpeI and SacII. Previously described *elavl3* (*HuC*) *cis*-regulatory elements (Higashijima et al. 2003) were placed upstream via LR recombination (Invitrogen) with an attL flanked *elavl3* entry clone. The resulting plasmid was then co-injected into 1-cell stage embryos at a concentration of 30 ng/μL with Tol2 transposase mRNA at a concentration of 30 ng/μL. A single founder was selected based on high and spatially broad expression. Outcrossing this founder generated 50% GCaMP6f-positive embryos, which were selected to establish the line.

Imaging

Zebrafish larvae (aged 5 - 10 dpf) were anaesthetized in mivacurium and embedded in low-melting temperature agarose (1.2-2.0 % in E3) in a glass-bottom dish (Mat Tek). They were imaged on a Nikon two-photon microscope (A1RMP), attached to a fixed stage upright microscope, using a 25x water immersion objective (NA = 1.1). The femtosecond laser (Coherent Vision II) was tuned to 920 nm for GCaMP imaging. Stacks were collected in resonant-scanning mode with a 525/50 nm bandpass emission filter and with 8x pixel averaging; single-plane images were collected in galvano-scanning mode with 2x pixel averaging. To image at 13 Hz , frames were collected using single-plane resonant-scanning mode without any pixel averaging. Fish were imaged during the day only, between 10 am and 7 pm. The facility lights were on from 8 am to 10 pm. Fish were selected at random for imaging.

Light stimuli were generated by 5 mm blue LEDs (458 nm peak emission). They were powered by a 5 V TTL signal from a control computer and synchronized with image capture using a National Instruments DAQ board, controlled by the Nikon Elements software. Light intensity at the sample was 0.13 mW/cm^2 unless otherwise stated.

For widefield microscopy, excitation was provided by LEDs (Cairn OptoLED) at

470 nm. Images were captured on a Zeiss Axio Examiner with a 40x water immersion objective, using an Evolve camera (Photometrics), by streaming with MetaMorph at 20 msec exposure time. The first frame was discarded to eliminate artifact from delay in shuttering, and ratio images were obtained by comparing each frame against the first frame of this time-stack using Fiji.

Data analysis

Data Preprocessing: Raw images obtained were first registered to correct for any vertical/horizontal movement artifacts using cross correlation. In case of high speed data using a resonant scanner, a median filter of size 3 was applied to remove noise. Non linear trends in the data were detrended using polynomials of order 2-5. Data was then normalized into Z-scores by subtracting the overall mean and dividing by the standard deviation. A rolling window average was then used to smooth noisy traces where necessary.

Pixel-Based analysis of Habenula and AF4: The Thunder platform (Freeman et al. 2014) was used for fast pixel based clustering and factorization. Principle Component Analysis was used for a low dimensional representation of the pixels to observe the population response to onset and offset of light. *K-means* clustering was performed to identify pixels with similar responses profiles. The scripts used for analysis are provided at this site.

Segmentation of Region of interest (ROI): To segment habenula cells, each stack was scaled 2x in imageJ for better segmentation. The enlarged stack was maximally projected to a single image, which was then subjected to a minimum filter and unsharp mask to sharpen the boundary of cells. ROIs were identified using the “find maxima…” command, as a way to localize regional darkest point as the center of each

ROI. The boundary of the ROI was outlined by “analyze particle…” that connects bright pixels into mosaic-like tessellated plane, encircling each darkest point. Each ROI was then numbered sequentially using the ImageJ ROI Manager and mapped back to the original despeckled image stack. Manual segmentation was done here to delete extraneous ROIs outside the habenula and to encircle cells that were not detected by the algorithm (<10% of total ROIs). In the last step, “Set measurements…” and “measure” in ImageJ provided the mean fluorescence value of all pixels within each ROI across the entire image stack and the x-y coordinates of each ROI. Time-lapse series in which dramatic z drifting occurred were excluded, as in this case ROIs could not be defined appropriately. To identify and verify light evoked responses seen in the pixel based analysis, K-means clustering (Figure 1G) was done on the activity traces from the segmented cells and neuropils following preprocessing from n=6 fish.

Neural tracing

DiD (Life Technologies) was dissolved in 50 µl ethanol to make a saturated solution. This was heated to 55˚C for 5 minutes prior to injection into the fish that had been fixed in 4% paraformaldehyde. Fish were mounted in 1.2% low melting temperature agarose dissolved in PBS. The dye was pressure injected into the habenula under a compound microscope (Leica DM LFS), using a 20X water immersion objective. For labeling the retina, a saturated solution of DiI in chloroform was used. Injections were carried out under a stereo microscope (Zeiss Stemi 2000). After injections, fish were stored at 4˚C overnight to allow tracing, and then imaged with a 40x water immersion objective on a Zeiss LSM 710 confocal microscope.

Antibody label

Larvae were fixed in 4% para-formaldehyde/PBS overnight at 4˚C. They were then

rinsed in PBS. The brains were dissected out, and permeabalized using 1% BSA (fraction V; Sigma), 0.1% DMSO and 0.1% Triton X-100. The antibodies used here, anti-vGlut1/2 (Synaptic Systems 135503; 1:100) and anti-GAD65/67 (Abcam ab11070; 1:500), have previously been used in zebrafish (A. Lee et al. 2010; Wyart et al. 2009). The brains were incubated in the primary antibody overnight, rinsed several times in PBS, then incubated in secondary antibody (Alexa 488 goat anti-rabbit; 1:1000). After washing, these were mounted in 1.2% agarose/PBS. Imaging was carried out using a Zeiss LSM 510 laser scanning confocal microscope, with a 40x water immersion objective.

Laser ablation

Tg(Elavl3:GCaMP6f) larvae were anaesthetized in mivacurium and then mounted in 2% low-melting temperature agarose. Lesions were created with the IR laser tuned to 960 nm. Lesioning was monitored by time-lapse imaging before and after each pulse, and was judged successful when there was a localized increase in GCaMP6f fluorescence, as well as the appearance of a gap in the tissue.

Figure legends

Figure 1. Neural activity in the habenula is altered by the light and darkness

(A) Dorsal view of a live 7 day-old fish, with GCaMP3 expression in the habenula (arrows) under the control of the *s1011tEt* GAL4 driver. (B) A single two-photon slice through the habenula of the fish in panel A. (C) A yz reconstruction at the point indicated by the yellow line in panel B. The dotted lines indicate imaging planes separated by 10 µm. The yellow line indicates the plane imaged in B. (D) Spatial distribution of major responses in the habenula. 5 planes are shown here. The colors are coded according to

the temporal pattern of response, as indicated in (E). Images were collected at a rate of 1 stack/second, and four light pulses were delivered for 20 seconds each, with variable inter-stimulus interval. The solid lines indicate light onset, while the dashed lines indicate light offset. (F) Trajectory of the habenula response in (D-E) is shown in two-dimensional state space, using the first two principal components (PC1 and PC2). Traces are color-coded according to the wedges in panel E. The bold lines correspond to light onset while the dashed lines are during periods of light OFF. (G) K-means cluster analysis of habenula response to pulses of blue light in 6 fish. Cells with excitation to light (top) or darkness (middle), or inhibition to light (bottom) were seen. Scale bar = 25 μm. a: anterior; p: posterior.

Figure 2. High-speed imaging identifies the dorsal left neuropil as the site of initial light- and dark-evoked responses in the habenula

(A-F) Dorsal view of a 5-day-old fish expressing GCaMP3 in the habenula, 250 milli-seconds (B), 500 milli-seconds (C), 1 second (D), 1.5 seconds (E), and 2 seconds (F) after the start of imaging using 20 Hz widefield fluorescence microscopy with 470 nm excitation. The arrowhead indicates the dorsal left neuropil. (G, H) Two-photon imaging of the dorsal habenula at 13 Hz. The onset of 0.13 mW/cm^2 blue light evoked activity in one region of the dorsal left neuropil (yellow arrowhead), while the offset triggered activity in another region (cyan arrowhead). Pixels are colour-coded according to the traces in panel H, which are derived by K-means clustering. The solid lines indicate onset of light, whereas the dashed lines indicate offset of light. (I, J) Habenula response to 0.20 mW/cm^2 blue light. Traces were derived by K-means clustering. a: anterior, p: posterior. Scale bar = 25 μm.

Figure 3. The parapineal is not essential for habenula excitation by blue light.

(A) A dorsal view of the habenula in an *Et(sqKR4)* larva, with the parapineal labeled by the transgene (yellow arrow). (B, C) The parapineal before (B) and after (C) laser ablation. (D, E) Heat maps showing activity in responding cells of the dorsal left habenula before (D) and after (E) parapineal lesion in one fish. (F). Percentage of cells with sustained response to blue light, before and after parapineal lesion, in 6 fish. r is the correlation coefficient.

Figure 4. The dorsal thalamus innervates the habenula

(A) Dorsal view of the forebrain of a *Et(SqKR11)* larva, in which habenula afferents from the entopeduncular nucleus are fluorescently labeled. The dorsal left neuropil (arrow) is more weakly labeled than other neuropils. (B) Dorsal view of the habenula of a *Et(SqKR11)* larva, following DiD injection into the dorsal neuropil of the left habenula. The parapineal (arrow) has been retrogradely labeled. Habenula afferents from the entopeduncular nucleus are labeled by the transgene, and shown in red here. (C) A deeper focal plane of the same fish, showing bilateral label in the thalamus (white arrows). A labeled cell in the entopeduncular nucleus is also indicated (yellow arrow). (D) Lateral view of another larva, in which the dorsal left neuropil had been injected with DiD. The retrogradely labeled thalamic neuropil (arrow) and neurons (arrowhead) are indicated. The entopeduncular nucleus is indicated by the yellow arrow. (F) A close up view of the neuropil retrogradely labeled by DiD (cyan), in a fish where retinal ganglion cells had been labeled with DiI (yellow). RGC axons intermingle with fibers from DiD-labeled cells innervating the neuropil. (G) Dorsal view of a 6-day-old fish, labelled with an anti-vGlut1/2, which marks glutamatergic pre-synapses. There is strong label in the dorsal left neuropil (arrowhead). (H) Dorsal view showing label with an anti-GAD65/67

antibody. Labeled puncta are visible in the dorsal left neuropil (arrowhead). No labeled cell bodies can be detected. (I) A *Tg(gad1b:RFP, vGlut2:GAL4, UAS:eGFP)* fish, with GABAergic cells indicated in magenta, and glutamatergic cells shown in green. Both cell types can be detected in the thalamus. The arrowhead indicates the region of the thalamus that is labeled in panel E. All panels except (G) are single optical sections. The image in panel C is 80 μm below that in B. Pa: pallium; OT: optic tract; Hb: habenula; Th: thalamus. Scale bar = 25 μm.

Figure 5. The zebrafish thalamus has non-overlapping responses to light and darkness

(A-C) Dorsal view of thalamus of a *Tg(elavl3:GCaMP6f)* fish, showing response to repeated pulses of blue light. The time-series was obtained by two-photon imaging at 13 Hz, and the colors are dominant clusters obtained using K-means as shown in (D-F). Three different focal planes were imaged in the same fish. The numbers at the lower right in panels (A-C) indicate depth below the dorsal left habenula neuropil. Blue light was delivered for 20 seconds, with an inter-stimulus interval of 20 seconds. Light onset is indicated by the solid line, while light offset is indicated by the dashed line. Responses are seen in the thalamic neuropil (arrowhead) and in neurons (arrows). (G) The habenula response in the same fish. Fewer habenula neurons are labeled in the *Tg(elavl3:GCaMP6f)* line, compared to the *s1011tEt,UAS:GCaMP3* line. (H) Lateral view of the left thalamus in another fish, showing responses to blue light and darkness. The anterior ventral region responds to light OFF, while blue light triggers excitation more posteriorly. Pixels are color-coded according to the traces in panel I, obtained using K-means. (J-M) Dorsal view of the thalamus, showing response to two different intensities of blue light. (J, K) Response to 0.13 mW/cm2; (L, M) response to 0.20 mW/cm2. (J, L) are colored according to the K-means clusters seen in (K, M). a: anterior; p: posterior; d: dorsal; v: ventral. Scale bar = 25 μm.

Author contribution

Experiments were designed by CRK, QL and SJ. CRK carried out two-photon imaging. SK developed software and analyzed imaging data. QL performed parapineal lesion and imaging. CK performed antibody label. DGCH and IHB generated the *Tg(elavl3:GCaMP6f)* transgenic line. SJ performed wide-field imaging, dye tracing and wrote the manuscript.

References

Agetsuma, M. et al., 2010. The habenula is crucial for experience-dependent modification of fear responses in zebrafish. *Nature neuroscience*, 13(11), pp.1354–1356.

Amo, R. et al., 2014. The habenulo-raphe serotonergic circuit encodes an aversive expectation value essential for adaptive active avoidance of danger. *Neuron*, 84(5), pp.1034–1048.

Aschoff, J., 1960. Exogenous and endogenous components in circadian rhythms. *Cold Spring Harbor symposia on quantitative biology*, 25, pp.11–28.

Baden, T. et al., 2016. The functional diversity of retinal ganglion cells in the mouse. *Nature*, 529(7586), pp.345–350.

Badia, P. et al., 1991. Bright light effects on body temperature, alertness, EEG and behavior. *Physiology & behavior*, 50(3), pp.583–588.

Bargmann, C.I. & Marder, E., 2013. From the connectome to brain function. *Nature methods*, 10(6), pp.483–490.

Bianco, I.H. & Engert, F., 2015. Visuomotor transformations underlying hunting behavior

in zebrafish. *Current biology : CB*, 25(7), pp.831–846.

Blackshaw, S. & Snyder, S.H., 1997. Parapinopsin, a novel catfish opsin localized to the parapineal organ, defines a new gene family. *The Journal of neuroscience : the official journal of the Society for Neuroscience*, 17(21), pp.8083–8092.

Buckley, P.F. et al., 2009. Psychiatric comorbidities and schizophrenia. *Schizophrenia bulletin*, 35(2), pp.383–402.

Burgess, H.A. & Granato, M., 2007. Modulation of locomotor activity in larval zebrafish during light adaptation. *The Journal of experimental biology*, 210(Pt 14), pp.2526–2539.

Burgess, H.A., Schoch, H. & Granato, M., 2010. Distinct retinal pathways drive spatial orientation behaviors in zebrafish navigation. *Current biology : CB*, 20(4), pp.381–386.

Burrill, J.D. & Easter, S.S., 1994. Development of the retinofugal projections in the embryonic and larval zebrafish (Brachydanio rerio). *The Journal of comparative neurology*, 346(4), pp.583–600.

Chellappa, S.L., Gordijn, M.C.M. & Cajochen, C., 2011. Can light make us bright? Effects of light on cognition and sleep. *Progress in brain research*, 190, pp.119–133.

Chen, T.-W. et al., 2013. Ultrasensitive fluorescent proteins for imaging neuronal activity. *Nature*, 499(7458), pp.295–300.

Cheng, R.-K., Krishnan, S. & Jesuthasan, S., 2016. Activation and inhibition of tph2 serotonergic neurons operate in tandem to influence larval zebrafish preference for light over darkness. *Scientific reports*, 6, p.20788.

Cragg, B.G., 1961. The connections of the habenula in the rabbit. *Experimental neurology*, 3, pp.388–409.

Crick, F. & Koch, C., 2003. A framework for consciousness. *Nature neuroscience*, 6(2), pp.119–126.

Díaz, C. & Puelles, L., 1992. Afferent connections of the habenular complex in the lizard Gallotia galloti. *Brain, behavior and evolution*.

Dreosti, E. et al., 2014. Left-right asymmetry is required for the habenulae to respond to both visual and olfactory stimuli. *Current biology : CB*, 24(4), pp.440–445.

Easter, S.S. & Nicola, G.N., 1996. The development of vision in the zebrafish (Danio rerio). *Developmental biology*, 180(2), pp.646–663.

Fisher, R.S. & Velasco, A.L., 2014. Electrical brain stimulation for epilepsy. *Nature reviews. Neurology*, 10(5), pp.261–270.

Freeman, J. et al., 2014. Mapping brain activity at scale with cluster computing. *Nature methods*, 11(9), pp.941–950.

Getting, P.A., 1989. Emerging principles governing the operation of neural networks. *Annual Review of Neuroscience*, 12, pp.185–204.

Hattar, S. et al., 2003. Melanopsin and rod-cone photoreceptive systems account for all major accessory visual functions in mice. *Nature*, 424(6944), pp.76–81.

Hendricks, M. & Jesuthasan, S., 2007. Asymmetric innervation of the habenula in zebrafish. *The Journal of comparative neurology*, 502(4), pp.611–619.

Higashijima, S.-I. et al., 2003. Imaging neuronal activity during zebrafish behavior with a

genetically encoded calcium indicator. *Journal of neurophysiology*, 90(6), pp.3986–3997.

Hikosaka, O., 2010. The habenula: from stress evasion to value-based decision-making. *Nature reviews Neuroscience*, 11(7), pp.503–513.

Jabeen, S. & Thirumalai, V., 2013. Distribution of the gap junction protein connexin 35 in the central nervous system of developing zebrafish larvae. *Frontiers in neural circuits*, 7, p.91.

Jhou, T.C. et al., 2009. The rostromedial tegmental nucleus (RMTg), a GABAergic afferent to midbrain dopamine neurons, encodes aversive stimuli and inhibits motor responses. *Neuron*, 61(5), pp.786–800.

Kanner, A.M., 2011. Anxiety disorders in epilepsy: the forgotten psychiatric comorbidity. *Epilepsy Currents*, 11(3), pp.90–91.

Kanner, A.M., 2003. Depression in epilepsy: prevalence, clinical semiology, pathogenic mechanisms, and treatment. *Biological Psychiatry*, 54(3), pp.388–398.

Kim, U. & Chang, S.-Y., 2005. Dendritic morphology, local circuitry, and intrinsic electrophysiology of neurons in the rat medial and lateral habenular nuclei of the epithalamus. *The Journal of comparative neurology*, 483(2), pp.236–250.

Kojima, D. et al., 2008. Differential expression of duplicated VAL-opsin genes in the developing zebrafish. *Journal of neurochemistry*, 104(5), pp.1364–1371.

Koyanagi, M. et al., 2015. Diversification of non-visual photopigment parapinopsin in spectral sensitivity for diverse pineal functions. *BMC Biology*, 13(1), p.1.

Krishnan, S. et al., 2014. The Right Dorsal Habenula Limits Attraction to an Odor in Zebrafish. *Current biology : CB*.

Lee, A. et al., 2010. The habenula prevents helpless behavior in larval zebrafish. *Current biology : CB*, 20(24), pp.2211–2216.

Lee, S.-H. & Dan, Y., 2012. Neuromodulation of Brain States. *Neuron*, 76(1), pp.209–222.

LeGates, T.A. et al., 2012. Aberrant light directly impairs mood and learning through melanopsin-expressing neurons. *Nature*, 491(7425), pp.594–598.

Marburg, O., 1944. The structure and fiber connections of the human habenula. *Journal of Comparative Neurology*, 80, pp.211–233.

Marder, E., 2012. Neuromodulation of neuronal circuits: back to the future. *Neuron*, 76(1), pp.1–11.

Mitchell, A.S. et al., 2014. Advances in Understanding Mechanisms of Thalamic Relays in Cognition and Behavior. *Journal of Neuroscience*, 34(46), pp.15340–15346.

Miyasaka, N. et al., 2009. From the olfactory bulb to higher brain centers: genetic visualization of secondary olfactory pathways in zebrafish. *The Journal of neuroscience : the official journal of the Society for Neuroscience*, 29(15), pp.4756–4767.

Morley, B.J., Spangler, K.M. & Javel, E., 1985. The development of somatostatin immunoreactivity in the interpeduncular nucleus of the cat. *Brain research*, 352(2), pp.241–248.

Mueller, T., 2012. What is the Thalamus in Zebrafish? *Frontiers in neuroscience*, 6, p.64.

Muller, J.E. et al., 2004. Anxiety disorders and schizophrenia. *Current Psychiatry Reports*, 6(4), pp.255–261.

Newman, J., 1995. Thalamic contributions to attention and consciousness. *Consciousness and cognition*, 4(2), pp.172–193.

Northcutt, R.G. & Wullimann, M.F., 1988. The visual system in teleost fishes: morphological patterns and trends. In J. Atema et al., eds. *Sensory Biology of Aquatic Animals*. pp. 515–552.

Okamoto, H., Agetsuma, M. & Aizawa, H., 2012. Genetic dissection of the zebrafish habenula, a possible switching board for selection of behavioral strategy to cope with fear and anxiety. *Developmental neurobiology*, 72(3), pp.386–394.

Portugues, R. et al., 2014. Whole-brain activity maps reveal stereotyped, distributed networks for visuomotor behavior. *Neuron*, 81(6), pp.1328–1343.

Proulx, C.D., Hikosaka, O. & Malinow, R., 2014. Reward processing by the lateral habenula in normal and depressive behaviors. *Nature neuroscience*, 17(9), pp.1146–1152.

Provencio, I., Rollag, M.D. & Castrucci, A.M., 2002. Photoreceptive net in the mammalian retina. This mesh of cells may explain how some blind mice can still tell day from night. *Nature*, 415(6871), p.493.

Quina, L.A. et al., 2014. Efferent Pathways of the Mouse Lateral Habenula. *The Journal of comparative neurology*.

Robles, E., Laurell, E. & Baier, H., 2014. The retinal projectome reveals brain-area-specific visual representations generated by ganglion cell diversity. *Current biology : CB*, 24(18), pp.2085–2096.

Satou, C. et al., 2013. Transgenic tools to characterize neuronal properties of discrete populations of zebrafish neurons. *Development (Cambridge, England)*, 140(18), pp.3927–3931.

Semm, P. & Demaine, C., 1984. Electrophysiology of the pigeon's habenular nuclei: evidence for pineal connections and input from the visual system. *Brain research bulletin*, 12(1), pp.115–121.

Sherman, S.M. & Guillery, R.W., 2002. The role of the thalamus in the flow of information to the cortex. *Philosophical Transactions of the Royal Society B: Biological Sciences*, 357(1428), pp.1695–1708.

Steenbergen, P.J., Richardson, M.K. & Champagne, D.L., 2011. Patterns of avoidance behaviours in the light/dark preference test in young juvenile zebrafish: a pharmacological study. *Behav Brain Res*, 222(1), pp.15–25.

Stephenson-Jones, M. et al., 2012. Evolutionary conservation of the habenular nuclei and their circuitry controlling the dopamine and 5-hydroxytryptophan (5-HT) systems. *Proceedings of the National Academy of Sciences of the United States of America*, 109(3), pp.E164–73.

Vandewalle, G. et al., 2010. Spectral quality of light modulates emotional brain responses in humans. *Proceedings of the National Academy of Sciences*, 107(45), pp.19549–19554.

Wang, R.Y. & Aghajanian, G.K., 1977. Physiological evidence for habenula as major link between forebrain and midbrain raphe. *Science (New York, NY)*, 197(4298), pp.89–91.

Ward, L.M., 2013. The thalamus: gateway to the mind. *Wiley Interdisciplinary Reviews: Cognitive Science*.

Wyart, C. et al., 2009. Optogenetic dissection of a behavioural module in the vertebrate spinal cord. *Nature*, 461(7262), pp.407–410.

Yañez, J. & Anadon, R., 1994. Afferent and efferent connections of the habenula in the larval sea lamprey (Petromyzon marinus L.): an experimental study. *The Journal of comparative neurology*, 345(1), pp.148–160.

Young, K.A. et al., 2000. Reduced number of mediodorsal and anterior thalamic neurons in schizophrenia. *Biological Psychiatry*, 47(11), pp.944–953.

Zhao, H. & Rusak, B., 2005. Circadian firing-rate rhythms and light responses of rat habenular nucleus neurons in vivo and in vitro. *Neuroscience*, 132(2), pp.519–528.

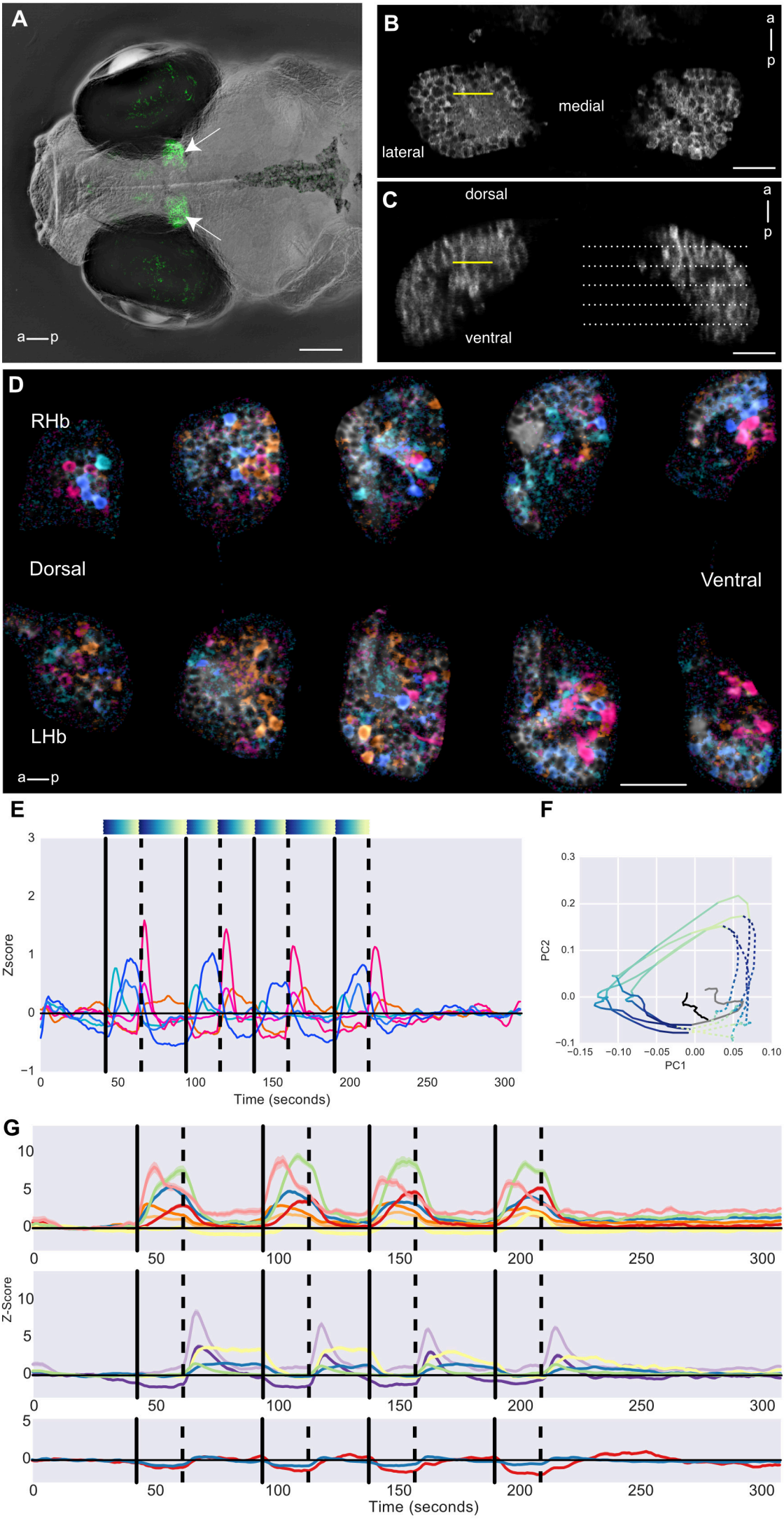
A
a—p
B
a
p
medial
lateral
C
dorsal
a
p
ventral
D
RHb
Dorsal
Ventral
LHb
a—p
E
Zscore
Time (seconds)
F
PC2
PC1
G
Z-Score
Time (seconds)

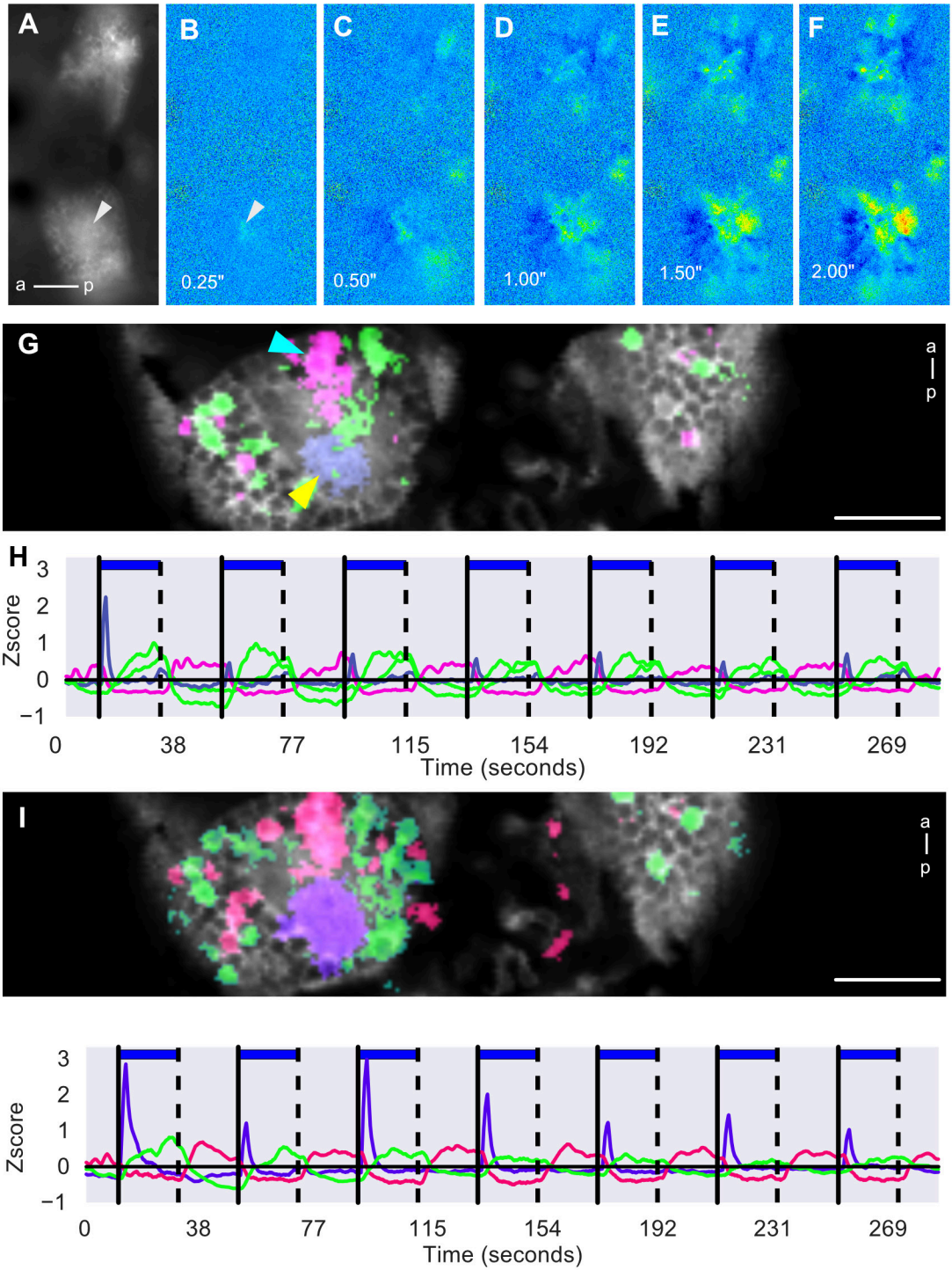
A
a
p
B
0.25"
C
0.50"
D
1.00"
E
1.50"
F
2.00"
G
a
p
H
Zscore
3
2
1
0
−1
0
38
77
115
154
192
231
269
Time (seconds)
I
a
p
Zscore
3
2
1
0
−1
0
38
77
115
154
192
231
269
Time (seconds)

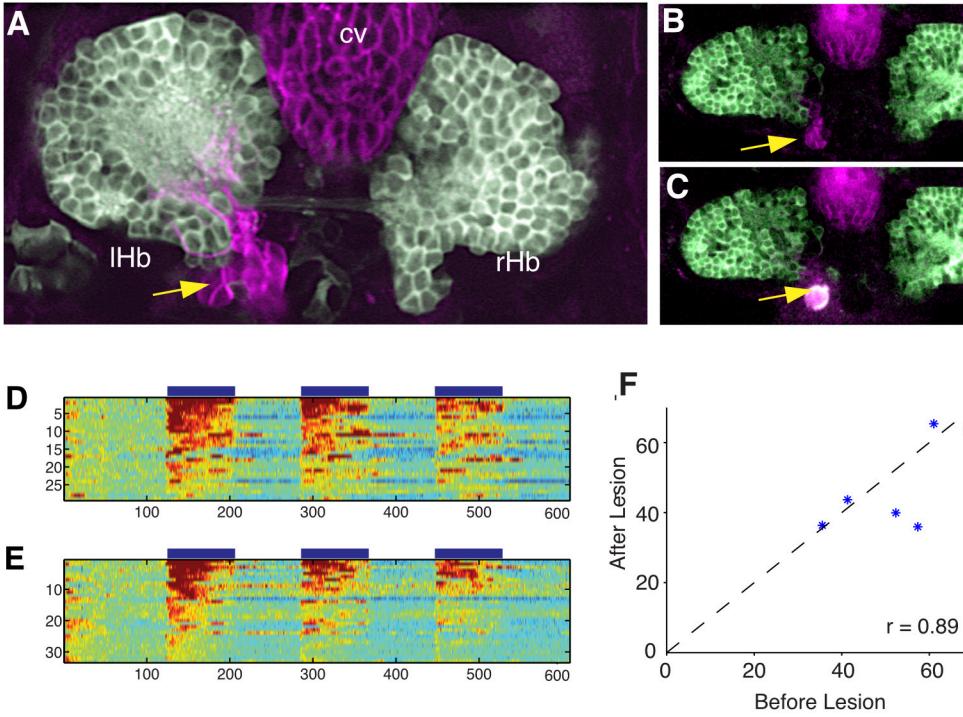
A
cv
lHb
rHb
B
C
D
5
10
15
20
25
100
200
300
400
500
600
E
10
20
30
100
200
300
400
500
600
F
After Lesion
Before Lesion
0
20
40
60
r = 0.89

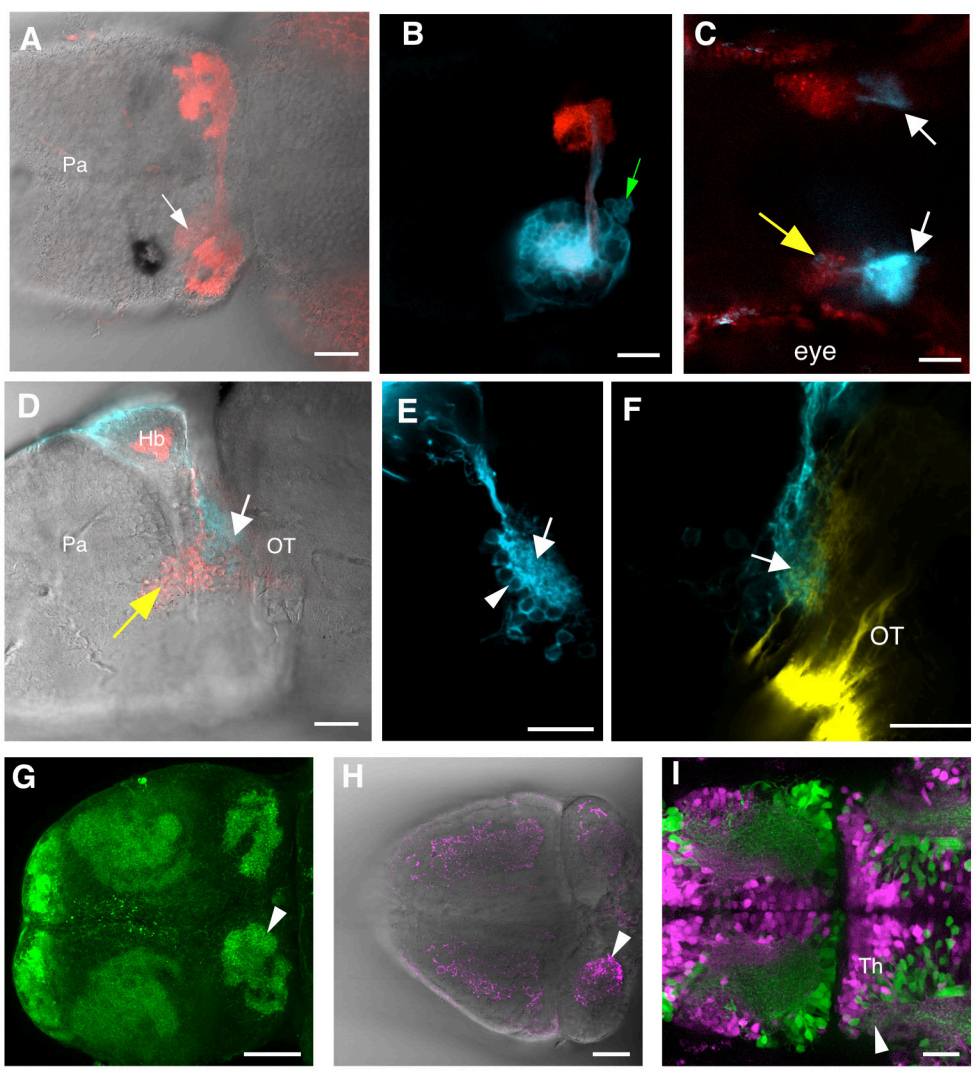
A
Pa
B
C
eye
D
Hb
Pa
OT
E
F
OT
G
H
I
Th

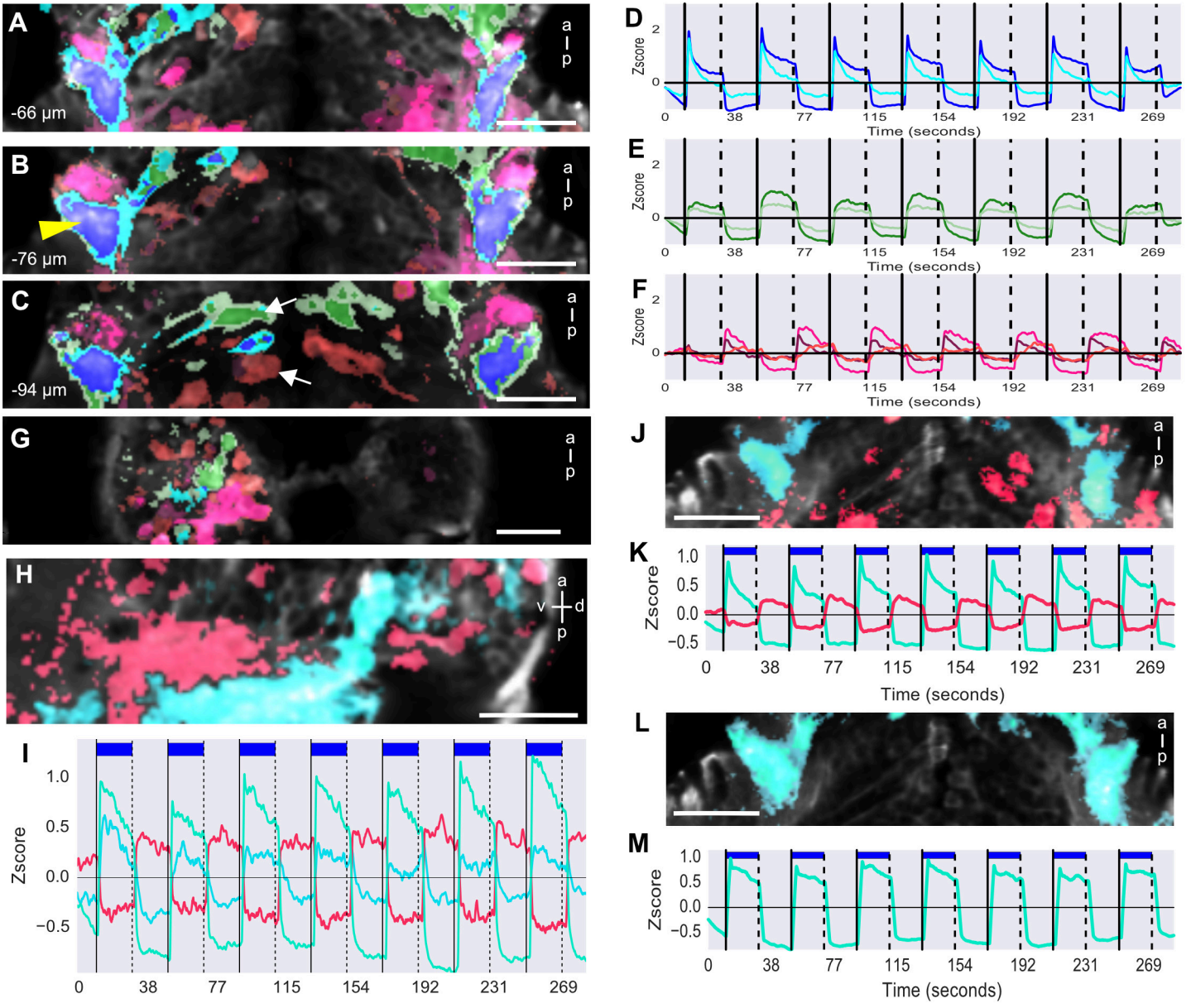
A
-66 µm
a
l
p
B
-76 µm
C
-94 µm
G
H
a
v
d
p
I
Zscore
1.0
0.5
0.0
−0.5
0
38
77
115
154
192
231
269
D
E
F
Zscore
2
0
Time (seconds)
J
K
L
M